Dynamic Modeling of Driver Control Strategy of Lane-Change Behavior and Trajectory Planning for Collision Prediction

Guoqing Xu, Li Liu, Yongsheng Ou, and Zhangjun Song

***Abstract*—This paper introduces a dynamic model of the driver control strategy of lane-change behavior and applies it to trajectory planning in driver-assistance systems. The proposed model reflects the driver control strategies of adjusting longitudinal and latitudinal acceleration during the lane-change process and can represent different driving styles (such as slow and careful, as well as sudden and aggressive) by using different model parameters. We also analyze the features of the dynamic model and present the methods for computing the maximum latitudinal position and arrival time. Furthermore, we put forward an extended dynamic model to represent evasive lane-change behavior. Compared with the fifth-order polynomial lane-change model, the dynamic models fit actual lane-change trajectories better and can generate more accurate lane-change trajectories. We apply the dynamic models in emulating different lane-change strategies and planning lane-change trajectories for collision prediction. In the simulation, we use the models to compute the percentage of safe trajectories in different scenarios. The simulation shows that the maximum latitudinal position and arrival time of the generated lane-change trajectories can be good indicators of safe lane-change trajectories. In the field test, the dynamic models can generate the feasible lane-change trajectories and efficiently obtain the percentage of safe trajectories by computing the minimum gap and time to collision. The proposed dynamic model and module can be combined with the human–machine interface to help the driver easily identify safe lane-change trajectories and area.**

***Index Terms*—Driving behavior, driver control strategy, dynamic model, lane change, trajectory planning.**

I. Introduction

MODELING driving behaviors and skills has attracted considerable attention from the developers of advanced driver-assistance systems (ADASs) and vehicle active safety system [1]. In [2], Lindgren *et al.* compare the driving cultures between China and Sweden. They point out that the ADAS should present meaningful and worthy information and driving culture is the key factor that enhances road safety. Therefore, it is important to integrate driving behavior models or control strategies into system designs to decrease driver's burden and enhance driving safety. The kernels of modeling driving behavior are efficiently emulating the driver control strategy and characterizing the driving style for different driving tasks [3]–[5].

Modeling the driver control strategy and recognizing different behavioral stages are highly valuable research directions in modeling driving behavior. Numerous methods and models have been proposed in various fields, from vehicle control to intelligent transportation systems (see Table I). In [6], Olson carries out comprehensive research on natural lane-change behavior and numerous analyses of its features and scenarios. Gipps [7] and Ahmed [8] use the gap acceptance model to represent longitudinal behavior before lane change is initiated. In [9], Kesting *et al.* propose minimizing overall braking induced by lane change (MOBIL) to derive lane-change rules. The two methods are used to model the lane-change decision-making process and are applied in traffic simulation. In [10], Oliver and Pentland use hidden Markov models (HMM) to recognize the lane-change state. They used different features to classify lane-keeping and lane-changing behaviors. In [11] and [12], Mandiala and Salvucci use support vector machines and "model tracking" to increase the performance of lane-change classifiers. In [13], McCall *et al.* employ the latitudinal position and head motion to infer lane-change intent. Their study shows the possibility of generating lane-change trajectories and predicts possible collisions before lane-change maneuvers are initiated. Although the aforementioned methods can recognize the different stages of lane-change behavior, as well as define when and where lane-change maneuver starts and ends, these approaches should be used in combination with methods of predicting driving trajectories to foresee impending collisions. In [14], Pentland and Liu develop an HMM with a set of dynamic models to recognize driving behavior and predict drivers' subsequent actions. However, the lane-change dynamic model is not provided. In [15], Salvucci uses cognitive architectures to analyze the relationship between the perceived visual factors and steering angle of lane-change behavior. In [16], Kim *et al.* use the piecewise polynomial model to represent different stages of lane-change behavior with different regression models and analyze lane-change styles of different drivers.

Manuscript received February 22, 2011; revised October 7, 2011 and January 16, 2012; accepted January 20, 2012. Date of publication March 6, 2012; date of current version August 28, 2012. This work was supported by in part by Shenzhen Key Laboratory of Electric Vehicle Powertrain Platform and Safety Technology under Grant CXB201005260057A and the Chinese Academy of Sciences through the Hundred Talents Program under Grant Y14406. The Associate Editor for this paper was A. Zelinsky.

G. Xu is with the Department of Electrical Engineering, Tongji University, Shanghai 200092, China, and also with Shenzhen Institute of Advanced Integration Technology, Chinese Academy of Sciences/The Chinese University of Hong Kong, Shenzhen 518055, China (e-mail: gq.xu@siat.ac.cn).

L. Liu, Y. Ou, and Z. Song are with Shenzhen Institute of Advanced Integration Technology, Chinese Academy of Sciences/The Chinese University of Hong Kong, Shenzhen 518055, China (e-mail: li.liu@sub.siat.ac.cn; ys.ou@siat.ac.cn; zj.song@siat.ac.cn).

Color versions of one or more of the figures in this paper are available online at http://ieeexplore.ieee.org.

Digital Object Identifier 10.1109/TITS.2012.2187447

TABLE I
METHODS AND MODELS OF ANALYZING LANE-CHANGE BEHAVIOR

Category	Research	Model or Method	Test platform	Object
Analyze natural lane-change behavior	Olsen[6]	Statistics analysis of natural lane-change data	Instrumental vehicle	Analyzing various features of natural lane-change behavior
Model lane-change decision behavior	Gipps[7] Ahmed[8] Kesting[9]	Hierarchical decision method and longitudinal dynamic model	Traffic data	Modeling the decision to consider a lane change and the decision to execute the lane change
Model and predict driver behavior(including lane-change behavior)	Pentland [14]	HMM and dynamic models	Driving simulator	Mapping from the sensory or perceptional information to the driver's decision making and operation
	Salvucci[15]	Cognitive architectures(ACR-T)		
	Kim[16]	PWP		
	Sekizawa[17]	SS-ARX		
	Tan[38]	A driver steering model based on the target angle error	Instrumental vehicle	
Recognize lane-change state	Oliver[10]	HMM	Instrumental vehicle	Classify lane-change state using various features
	Mandalia[11]	SVM		
	Salvucci[12]	A computational model		
Infer lane-change intent	McCall[13]	Sparse Bayesian learning	Instrumental vehicle	Infer lane-change intent using vehicle lateral position and driver head position
Generate lane-change trajectory	Enke[19]	A sinusoidal model	Simulation	Generating ideal lane-change trajectories
	Choven[20]	A sinusoidal model and a trapezoidal model		Generating evasive lane-change trajectories
	Nelsom[21] Papadimitri[22]	A fifth-order polynomial model		Generating smooth lane-change trajectories
Analyze safe and unsafe lane changes	Choven[20]	A sinusoidal model and trapezoidal model	Simulation	Analysis of lane change crashes
	Bascunana[23]	A longitudinal dynamic models		Analysis of lane change crashes
	Jula[24]	A longitudinal dynamic models with a latitudinal sinusoidal model		Analyze the minimum safe space of lane change
	Smith[25]	Statistics analysis of the natural lane-change data	Instrumental vehicle	Analysis of the safe or dangerous states of lane change
	Schubert[26] Broadhurst[27]	Probability model of lane-change maneuver	Instrumental vehicle	Assess traffic situation for lane change

In [17], Sekizawa *et al.* apply the stochastic switched autoregressive exogenous model to the modeling and recognition of lane-change behavior of different drivers. The two models both monitor the driver's operation and perception and use different regression models of control strategy to model different stages of lane-change behavior. In [38], the driver steering action is modeled based on the target head error for double lane change. The preview target points and vehicle current heading angle are needed to compute the target head error. The aforementioned methods share similar problems. First, these methods are too complicated to clearly clarify physical meanings. They attempt to incorporate every possible or perceptional factor into the lane-change behavior model. Hence, the trained model always approximates a black box with various locks. Adjusting the model parameters in accordance with different driving styles is difficult to accomplish. Second, most of these methods require fitting to the collected dataset and offline learning of the model parameters. The learning process is always complex and time consuming because of the numerous model parameters and slow convergence of the search algorithm.

Modeling the driver control strategy and predicting lane-change trajectories using a dynamic model with some measurable and limited parameters is an attractive and feasible method. The advantages of dynamic model are that it can usually (not always) effectively explain causality with differential equations and increase our understanding of driving behavior. In the applications of driver-assistance systems, the dynamic model can more efficiently plan safe and feasible lane-change trajectories than other models. In [18], Siedge and Marshek compare different models for generating ideal lane-change trajectories. In [19], Enke uses the sinusoidal function to model normal lane-change behavior. This model has extensively been analyzed in different fields. In [20], the sinusoidal and trapezoidal functions are used to describe lane-change maneuvers for analyzing lane-change crashes. However, fitting the different restrictions of lane-change behavior by adjusting model parameters is difficult. In [21] and [22], the lane-change trajectory is generated by a fifth-order polynomial. Although the method can generate a smooth lane-change path, the generated trajectory is fixed when the initial and final vehicle states are fixed. Therefore, it does not correspond to actual lane-change trajectories, and the method cannot effectively predict impending collisions.

Furthermore, the lane-change model should generate feasible and safe trajectories, as well as predict potential collisions for driver-assistance systems. In [23], Bascunana analyzes the dynamic conditions of safe and unsafe lane changes between

related vehicles. The lane-change trajectory is generated according to a sinusoidal function. In [24], Jula *et al.* examine different longitudinal acceleration models to determine safe and unsafe regions, as well as minimum longitudinal safe spacing between vehicles and surrounding automobiles for lane-change scenarios. In [25], Smith *et al.* use four states to efficiently label the severity level of lane-change behavior according to relative longitudinal distance and speed. In [26], Schubert *et al.* employ different vehicle sensors to detect the driving environment and assess the safety of lane-change maneuvers based on a Bayesian network. In [27], different dynamic models of traffic participants are analyzed, and Monte Carlo sampling is applied to compute the collision probability. The method can simulate possible traffic participants' behaviors and assess dangerous or safe areas with collision probability. However, because of the countless options and improper prior distribution of the control input, the collision probability results sometimes considerably deviate from the appropriate or expected value. Therefore, the efficient generation of different types of trajectories and the computation of time to collision (TTC) and minimum gaps by a lane-change model will be highly useful for correctly predicting potential collisions in driver-assistance systems.

This paper focuses on modeling lane-change behavior as a dynamic model and planning safe and feasible lane-change trajectories between a test vehicle and other traffic participants. Using the model, we aim at clearly describing different driving styles and efficiently generating lane-change trajectories. Finally, our lane-change assistance system, which uses the dynamic model, can help drivers more accurately plan lane-change trajectories and predict collisions. Therefore, the lane-change dynamic model is not used to autonomously and smoothly control a vehicle as it changes lanes. We propose a dynamic lane-change model that reflects the driver control strategy of adjusting longitudinal and latitudinal acceleration. We then use the lane-change and generic dynamic models to generate the trajectories for the test vehicle and other traffic participants. Finally, we compute the TTC and minimum gaps for every lane-change trajectory to identify safe lane-change trajectories and alert the driver of dangerous situations.

The rest of this paper is organized as follows. Section II introduces the proposed measurements and lane-change data preprocessing and filtering. Section III presents the framework of our driver-assistance system and lane-change module. Section IV analyzes lane-change dynamic models and their features. The several control strategies with the dynamic model are given. Section V describes the dynamic models of other participants and the generation of safe and feasible lane-change trajectories. Section VI discusses the experiments and results, including the comparison of the dynamic modes and fifth-order polynomial models. The field test and simulation of the lane-change module are also presented. Section VII presents the discussion and conclusion.

II. Measurements

A. Test Vehicle and Sensors

We collect lane-change data from the test vehicle with different vehicle sensors and the Real Time Kinematic Differential–Global Position System (RTK-DGPS) X90 from HuaCe Navigation Technology Ltd. The location of the vehicle sensors and RTK-DGPS receiver are shown in Fig. 1. We extracted the velocity information of test vehicles from a controller area network (CAN). The velocity information comes from the vehicle control unit of an electrical vehicle, which also provides velocity information to the speedometer by the CAN. We detect the steering angle of the vehicle's front wheel based on a rope displacement sensor PLD-10-V from Shenzhen PonReed Technology Ltd. The output of the sensor and the steering angle of the front wheel has been calibrated using an automobile front wheel steering angle detector.

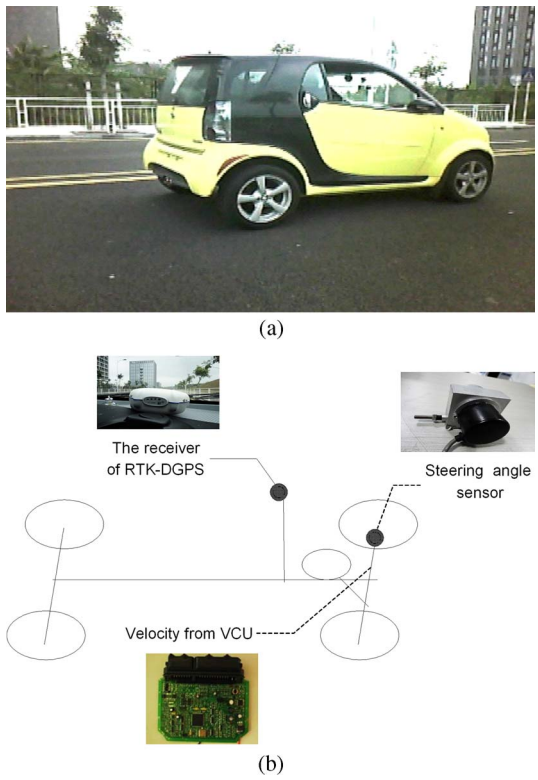

Fig. 1. Test vehicle and the sensors. (a) Test vehicle. (b) Vehicle sensors.

RTK-DGPS is reported to be of decimeter-level accuracy in the experimental environment and test vehicle in high speed (40–60 km/h). The position accuracy of the trajectory depends on several factors such as the accuracy of the digital map and the number of satellites located by the system. When seven or eight satellites can be located by the RTK-DGPS receiver and the vehicles move along a known straight lane/line in the test track, the average error of the trajectory is 0.2 m compared with the line in the local digital map. The vehicle sensors and the receiver of RTK-DGPS were both updated at 5 Hz. The steering angle sensor noise has a 3° standard deviation. All the data are recorded and transferred to a laptop personal computer.

In [28] and [29], the different sensors and methods for estimating vehicle position and filtering driving trajectories are described and compared. With regard to lane-change behavior, the duration time is always short, and the latitudinal displace is narrow. Hence, we fuse RTK-DGPS information with the velocity and steering angle from the vehicle sensors to estimate lane-change trajectories.

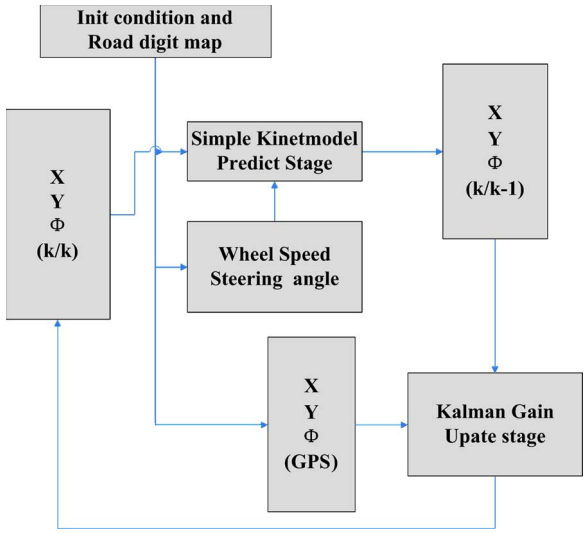

Fig. 2. Extended Kalman filter process.

B. Extended Kalman Filter and Coordinate

We use the first-order extend Kalman filter to estimate the vehicle position and reconstruct the trajectories on the test tracks. Fig. 2 shows the process of estimating vehicle position combining the DGPS and the vehicle sensors used in [28] and [29]. The coordinate of the Global Positioning System Universal Transverse Mercator (GPS UTM) is used in the process.

The prediction block applies a simple kinematics model. In the predicting process, the vehicle state at time k is estimated based on the vehicle state at time $k-1$ and the vehicle sensors at time k. The kinematics model is

$$\begin{bmatrix} \dot{x} \\ \dot{y} \\ \dot{\phi} \end{bmatrix} = \begin{bmatrix} V \cdot \cos(\phi) \\ V \cdot \sin(\phi) \\ \frac{V}{L} \cdot \tan(angle) \end{bmatrix} \tag{1}$$

where *angle* is the front-wheel steering angle, V is the vehicle's wheel speed, L is the axis length, and ϕ is the yaw angle at the GPS UTM coordinate. The GPS position is represented in UTM format. The predicted state $\overline{m(k)}$ is given by

$$\overline{m(k)} = \begin{bmatrix} x(k) \\ y(k) \\ \phi(k) \end{bmatrix} = \begin{bmatrix} x(k-1) + V \cdot \cos\left(\phi(k-1)\right) \Delta t \\ y(k-1) + V \cdot \sin\left(\phi(k-1)\right) \Delta t \\ \phi(k-1) + \frac{V}{L} \cdot \tan(angle) \Delta t \end{bmatrix}. \tag{2}$$

The estimate covariance $\overline{P}(k)$ is updated by

$$\begin{aligned} \overline{P(k)} &= F_x(m(k-1), k-1) \overline{P(k-1)} F_x^T \left(m(k-1), k-1\right) \\ &\quad + Q(k-1) \\ F_x(m(k-1), k-1) &= \left. \frac{\partial f_j(x, k-1)}{\partial \mathrm{x_j}} \right|_{x=m} \\ &= \begin{bmatrix} 1 & 0 & -V \sin\left(\phi(k-1)\right) \\ 0 & 1 & V \cos\left(\phi(k-1)\right) \\ 0 & 0 & 1 \end{bmatrix}. \end{aligned} \tag{3}$$

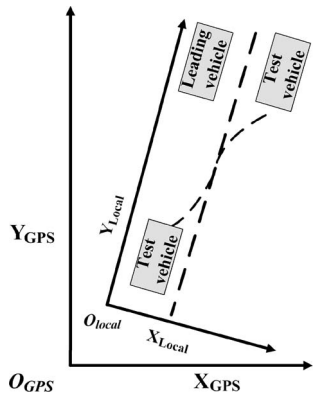

Fig. 3. Coordinate transformation.

The update block estimates the measurement residual $r(k)$ and covariance $S(k)$, as well as the Kalman gain $K(k)$ at time k combined with the observation of vehicle state, i.e.,

$$\begin{aligned} r(k) &= y(k) - H\left(\overline{m(k)}, k\right) \\ S(k) &= H_x\left(\overline{m(k)}, k\right) \overline{P(k)} H_x^T\left(\overline{m(k)}, k\right) \\ K(k) &= \overline{P(k)} H_x^T\left(\overline{m(k)}, k\right) S^{-1}(k) \\ H &= \begin{bmatrix} 1 & 0 & 0 \\ 0 & 1 & 0 \end{bmatrix}. \end{aligned} \tag{4}$$

Finally, the results of vehicle position $\overline{m(k)}$ at time k are given based on the measurement residual $r(k)$, vehicle predicted status $\overline{m(k)}$, and the Kalman gain $K(k)$ as

$$\begin{aligned} m(k) &= \overline{m(k)} + K(k) r(k) \\ P(k) &= \overline{P(k)} - K(k) S(k) K^T(k). \end{aligned} \tag{5}$$

The rotation transformation from the coordinate of UTM to the local coordinate is

$$\begin{bmatrix} X_{local} \\ Y_{local} \end{bmatrix} = \begin{bmatrix} \cos\theta & -\sin\theta \\ \sin\theta & \cos\theta \end{bmatrix} \begin{bmatrix} X_{gps} \\ Y_{gps} \end{bmatrix} \tag{6}$$

where θ is the angle between the x-axes of UTM and the x-axis of the local coordinate, as shown in Fig. 3. The local coordinate is defined in the test track's digital map.

C. Data Collection

The first step of modeling lane-change behavior is collecting measurable data on driving environment, driver, and vehicle. Although different types of sensors have different sampling rates, the data should be collected at a fixed sample rate. We select the low sampling rate of the sensor as the system sampling rate. We use the interpolation to align the data according to timestamp to avoid timestamp mismatch in offline processing.

For the lane-change applications, we record the test vehicle position and speed, as well as the longitudinal distance between the test and leading vehicles or other traffic participants on the current or destination lane. The longitudinal and latitudinal positions and speed of the test vehicle can be obtained using

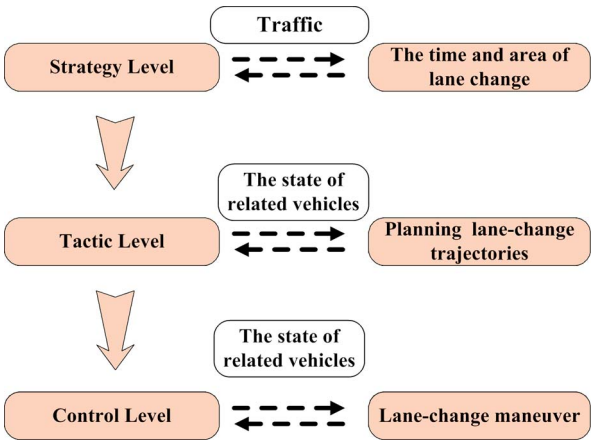

Fig. 4. Levels of lane-change behavior.

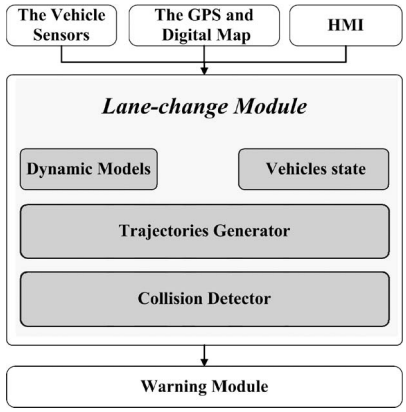

Fig. 5. Lane-change module.

a RTK-DGPS receiver and vehicle sensors. The gap between the test vehicle and leading traffic participants can be obtained using a laser sensor. Because the positions of the other traffic participants in the destination lane are difficult to obtain, their positions and speeds are determined using the RTK-DGPS receiver and the sensors located in the other traffic participants. Finally, the data can wirelessly be transferred to the laptop in the test vehicle for real-time analysis.

III. System Description

A. Lane-Change Behavior and System Design

Driving behavior is the dynamic, stochastic, and interactive process among the driver, vehicle, and driving environment. In [30], driving behavior is considered to proceed at three levels. Following this idea, lane-change behavior is one type of driving behaviors and can also be divided into the following three levels (see Fig. 4).

1) Level 1 corresponds to the strategy level and pertains to the ability to perceive the current driving environment. In this stage, the driver assesses the traffic environment for a feasible lane change. The driver gathers different information such as the other vehicles or obstacles in the destination and current lane, lane layout, and lane markings. The available lane-change time and area are determined. During the process, the driver remains in the lane-keeping state.
2) Level 2 corresponds to the tactical level. It transforms and decomposes the goal or complex driving task into several easy-to-implement subtasks such as lane keeping with different acceleration or deceleration and lane change. In this stage, the driver generates lane-change trajectories and checks whether the trajectories are feasible. The collision time is predicted according to the state of related vehicles and the planned lane-change trajectories. During the process, the driver determines the exact time at which the lane-keeping state changes into the lane-changing state. The turn signal is also flashed to notify the other vehicles.
3) Level 3 is the control level. It corresponds to maneuvering skills such as turning the steering wheel and pressing the throttle or brake to keep the vehicle moving along the planned trajectory. In this stage, the driver attempts to steadily and smoothly move the vehicle into the destination lane.

The design of the driver-assistance system and lane-change module should be based on the driver behavior to define the function and restriction of our driver-assistance system and improve the driving safe and driver acceptance. Our system is designed as an early warning system and corresponds to a portion of the strategic and tactical levels.

In the strategy level, the system uses the digital map, wireless data radio, and RTK-DGPS receiver to detect the driving environment and other vehicles states. The time and area of lane change is decided by the driver.

In the tactic level, when the system detects lane-change behavior by a turn signal or other features, the lane-change module will be triggered to predict the lane-change trajectories and plan safe trajectories.

In the control level, the system does not interfere with the driver control and only assesses the current maneuver during the lane change. The warning module assesses the situation and gives the warning signal according to the output of the lane-change module and other modules of the system.

B. Lane-Change Module

The framework of our lane-change module in the driver assistance system is shown in Fig. 5. The module has the following four parts:

- the states of related vehicles (including the driver's maneuvers in test vehicle);
- driving behavior models (dynamic models);
- a trajectory generator;
- a collision detector.

One essential part of a lane-change assistance system is the detection of the driver's lane-change intent or state to activate the lane-change module. In [31], Hetrick provides different rules for triggering the lane-change warning system. Different indicators are suggested to determine when lane change is initiated. Such indicators include the latitudinal position, steering angle of front wheel, and turn signal. In our system, the

lane-change module is mainly activated in the following three ways:

- the turn signal;
- the latitudinal position in the current lane and the steering angle of the front wheel (not used in test tracks with high curvature);
- the relative distance and velocity between the leading vehicle and the test vehicle.

When the sensor's data exceed the predefined thresholds, the lane-change module is automatically activated.

IV. Lane-Change Dynamic Model

In this part, we focus on modeling the driver's control strategy using dynamic models and analyze their features.

A. Lane-Change Control Strategy

The definition of lane change is a precondition of modeling the lane-change control strategy. In [32], Wierwille described a lane change in the following three stages:

1) the time and distance of adjusting the head between the current latitudinal position and the separation line of the current and destination lanes;
2) the time and distance of approaching and crossing the separation line;
3) further adjustments to ensure that the vehicle moves into the appropriate latitudinal position in the destination lane.

In [20], Chovan defines lane change as encompassing the following three stages:

1) turning the steering wheel to avoid crashing or to initiate lane change;
2) reverse action to adjust the latitudinal speed and vehicle heading;
3) further adjustments to ensure that the vehicle moves into the appropriate latitudinal position in the destination lane.

For latitudinal control, we assume that the driver assessed the following two factors: 1) whether the test vehicle has reached the target latitudinal position and 2) whether the vehicle can smoothly move into the target position at the current latitudinal speed. The process can also comprise the following three stages.

1) The driver increases the latitudinal speed to move away from the current lane. The driver turns the steering wheel and increases the latitudinal acceleration fast when the latitudinal gap is large, and vice versa.
2) The driver decreases the latitudinal acceleration when the latitudinal speed of the vehicle is too high and the vehicle cannot steadily move into the destination lane.
3) The driver adjusts the latitudinal acceleration to keep the latitudinal speed at 0 when the vehicle arrives at the target latitudinal position.

Further adjustments are implemented when overshooting occurs. That is, the vehicle moves away from the target latitudinal position when it arrives at this destination.

B. Dynamic Model

According to the proposed control strategy of lane-change behavior, we design a simple data fusion unit to estimate the latitudinal acceleration $ddq(t)$ based on the linear combination of latitudinal gap β-$q(t)$ and latitudinal speed $dq(t)$, i.e.,

$$ddq(t+\tau) = m \cdot (\beta - q(t)) - n \cdot dq(t) \tag{7}$$

where m, n, are the driver sensitivity of the latitudinal gap and latitudinal speed, respectively. They are always large than 0. β is the target latitudinal position, $q(t)$ is the current latitudinal position, and β-$q(t)$ is the latitudinal gap. τ is the delay time of driver control. In the actual lane-change process, latitudinal acceleration changes from 0 to the peak latitudinal acceleration in a short time.

During lane change, the longitudinal acceleration, in general, depends on the relative speed between the test vehicle and leading traffic participant in the current lane proposed in [33]–[35]. However, the duration time of lane change is relatively short, and the driver usually has prepared for a while before lane change is initiated. Hence, the variance of the longitudinal speed is small, and the gap between the test vehicle and leading traffic participants have less impact on the longitudinal speed observed. Therefore, we derive the longitude acceleration as follows:

$$dds(t+\tau) = -p \cdot dq(t) \tag{8}$$

where p reflects that the longitudinal acceleration depends on the latitudinal speed during the lane change. When the wheel velocity of test vehicle is fixed or the change is relative small, it is given by

$$\begin{aligned}
&ds_{t(n)} - ds_{t(n-1)} \\
&\quad = V\sin\left(\phi_{t(n)}\right) - V\sin\left(\phi_{t(n)} - \Delta\phi\right) \\
&\quad = V\sin\left(\phi_{t(n)}\right)(1-\cos\Delta\phi) + V\cos\left(\phi_{t(n)}\right)\sin(\Delta\phi) \\
&\quad \approx V\sin\left(\phi_{t(n)}\right)\left(\frac{\Delta\phi^2}{2!}\right) + dq\left(\Delta\theta - \frac{\Delta\phi^3}{3!}\right) \\
&\quad = dq\cdot\Delta\phi + V\sin(\phi_{t(n)})\left(\frac{\Delta\phi^2}{2!}\right) - dq\cdot\frac{\Delta\phi^3}{3!} \\
&\quad \approx dq\cdot\Delta\phi
\end{aligned} \tag{9}$$

where ϕ is the yaw angle of test vehicle, V is the wheel speed of the test vehicle, and $ds_{t(n)}$ is the longitudinal speed at time $t(n)$. The step $t(n) - t(n-1)$ is small, and $\Delta\phi \ll 1$.

In this model, we do not take the other traffic participants in the destination lane into account, because the collision detector module can detect dangerous trajectories by computing the gap between the trajectory and other participants on the lanes in Section IV. Therefore, the lane-change dynamic model of test vehicle is given as follows:

$$\begin{cases} ddq(t+\tau) = m\cdot(\beta - q(t)) - n\cdot dq(t) \\ dds(t+\tau) = -p\cdot dq(t). \end{cases} \tag{10}$$

For the parameter estimation of the model, we use the method of least mean square error to estimate the model's parameters. A residual function is defined as the difference between the trajectories generated by the model and the real lane-change trajectories.

Maximum Latitudinal Position: To generate lane-change trajectories and analyze the maximum latitudinal position, we simplify the dynamic model. The change of longitudinal speed and the delay time of the driver control are set to be zero. Therefore, the longitudinal speed is unchanged, and the dynamic model (10) is simplified to

$$\begin{cases} ddq(t) = m \cdot (\beta - q(t)) - n \cdot dq(t) \\ dds(t) = 0. \end{cases} \tag{11}$$

When the initial latitudinal position $q(0)$ is 2.5 m, the initial latitudinal speed $dq(0)$ is 0, and the target latitudinal position β is 5.5. The explicit solution of lane-change trajectory is as in (12), shown at the bottom of the page. The different initial latitudinal position $q(0)$ and the target latitudinal position β result in different solutions of lane-change trajectory. They are set by the driver or are learned from prerecorded data. The empirical value of the initial latitudinal position ranges from 1.5 m to 2.5 m. The empirical value of the target latitudinal position ranges from 4.5 m to 6 m. The explicit solution of latitudinal speed is

$$\begin{aligned} dq(t) &= \frac{\left(\frac{n}{2} - \frac{\sqrt{n^2-4m}}{2}\right)\left(3n + 3\sqrt{n^2-4m}\right)}{2e^{t\left(\frac{n}{2}\sqrt{\frac{n^2-4m}{2}}\right)}\sqrt{n^2-4m}} \\ &\quad - \frac{\left(\frac{n}{2} + \frac{\sqrt{n^2-4m}}{2}\right)\left(3n - 3\sqrt{n^2-4m}\right)}{2e^{t\left(\frac{n}{2}+\frac{\sqrt{n^2-4m}}{2}\right)}\sqrt{n^2-4m}} \\ &= \frac{6m\sinh\left(\frac{\sqrt{n^2-4m}}{2}t\right)}{e^{\frac{nt}{2}}\sqrt{n^2-4m}} = \frac{6m\left(-i\sin(i\cdot\frac{\sqrt{n^2-4m}}{2}t\right)}{e^{\frac{nt}{2}}\sqrt{n^2-4m}} \\ &= \begin{cases} \frac{6m\left(\sin\left(\frac{\sqrt{4m-n^2}}{2}t\right)\right.}{e^{\frac{nt}{2}}\sqrt{4m-n^2}}, & n^2-4m<0 \\ & n>0, m>0, t>0 \\ \frac{6m\left(\sinh\left(\frac{\sqrt{n^2-4m}}{2}t\right)\right.}{e^{\frac{nt}{2}}\sqrt{n^2-4m}}, & n^2-4m\geq 0 \\ & n>0, m>0, t>0. \end{cases} \end{aligned} \tag{13}$$

When the test vehicle arrives at the maximum latitudinal position, the latitudinal speed should be zero. Because the $exp(nt/2)$ and $sinh(t)$ is a monoincreasing variable with the time increasing, when the latitudinal speed is zero, the time is

$$t = \begin{cases} \infty, & n^2-4m \geq 0, m>0, n>0 \\ \frac{2\pi}{\sqrt{4m-n^2}}, & n^2-4m<0, m>0, n>0. \end{cases} \tag{14}$$

When $n^2-4m<0$, $m>0$, and $n>0$, we derive the maximum latitudinal position $mlatpos$ as

$$mlatpos = \frac{3}{e^{\frac{\pi n}{\sqrt{4m-n^2}}}} + 5.5. \tag{15}$$

When $n^2-4m \geqslant 0$, $m>0$, and $n>0$, we derive the maximum latitudinal position as

$$mlatpos = 5.5, n^2-4m \geq 0, m>0, n>0, t->\infty. \tag{16}$$

Stability Analysis: Here, we focus on analyzing the stability of the latitudinal acceleration equation. When the delay time is zero, the Laplace transformation of (7) is

$$Q(s) = \frac{m\beta}{s^2+ns+m} = \frac{m\beta}{\left(s+\frac{n-\sqrt{n^2-4m}}{2}\right)\left(s+\frac{n+\sqrt{n^2-4m}}{2}\right)}. \tag{17}$$

The characteristic roots of (17) should have negative real parts when (17) is stable. When $n^2-4m \geqslant 0$, $m>0$, and $n>0$, the characteristic roots have

$$\begin{cases} \frac{-n-\sqrt{n^2-4m}}{2} < 0 \\ \frac{-n+\sqrt{n^2-4m}}{2} < 0 \end{cases} \Rightarrow \frac{-n+\sqrt{n^2-4m}}{2} < 0 \Rightarrow m>0. \tag{18}$$

When $n^2-4m<0$, $m>0$, and $n>0$, the two real parts of characteristic roots, $-n+i\sqrt{4m-n^2}/2$, $-n-i\sqrt{4m-n^2}/2$, also have negative real parts. Therefore, (17) is stable when m and n are both larger than zero.

C. Generated Lane-Change Trajectories

To generate a safe and feasible lane-change trajectory or area, the parameters of the lane-change model are restricted. The restrictions of the model's parameter and features are listed as follows (some of the lane-change behavior's restrictions can be found in [6], [20], and [36]).

- The initial latitudinal position $q(0)$ is 2.5 m, the initial latitudinal speed $dq(0)$ is 0, and the target latitudinal position β is 5.5 m.
- The maximum latitudinal position $mlatpos$ is less than 6.5 m and larger than 5.5 m.

$$\begin{cases} \mathrm{s(t)} = \mathrm{v(0)} \cdot \mathrm{t} \\ q(t) = \frac{(2\beta-5)\left(n-\sqrt{n^2-4m}\right)}{4e^{t\cdot\left(\frac{n+\sqrt{n^2-4m}}{2}\right)}\sqrt{n^2-4m}} - \frac{(2\beta-5)\left(n+\sqrt{n^2-4m}\right)}{4e^{t\cdot\left(\frac{n-\sqrt{n^2-4m}}{2}\right)}\sqrt{n^2-4m}} + \beta \\ \quad = \frac{3n-3\sqrt{n^2-4m}}{2e^{t\cdot\left(\frac{n+\sqrt{n^2-4m}}{2}\right)}\sqrt{n^2-4m}} - \frac{3n+3\sqrt{n^2-4m}}{2e^{t\cdot\left(\frac{n-\sqrt{n^2-4m}}{2}\right)}\sqrt{n^2-4m}} + 5.5 \end{cases} \tag{12}$$

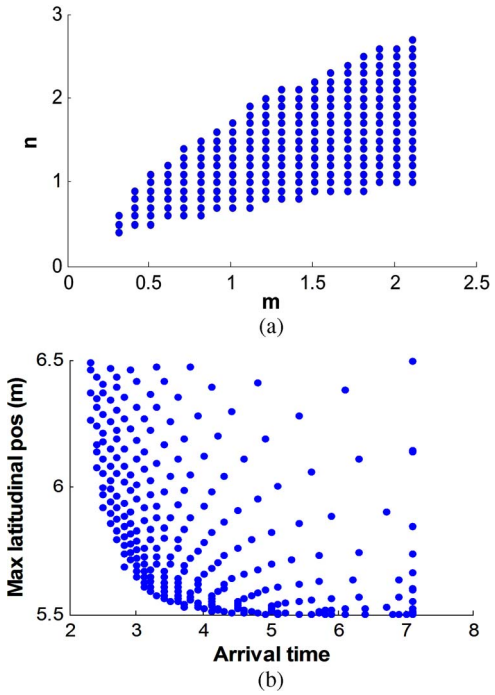

Fig. 6. Distribution of the model's parameters. (a) Distribution of the model's parameters. (b) Maximum latitudinal position and the arrival time.

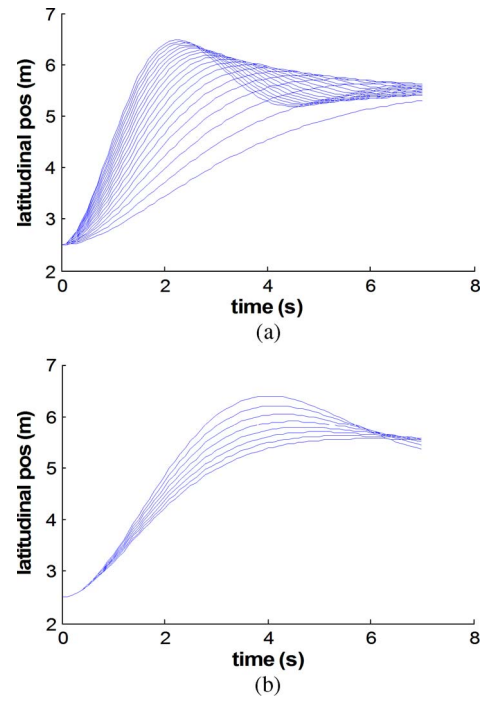

Fig. 7. Generated trajectories. (a) n is fixed to 1, and m is from 0.3 to 2.2. (b) m is fixed to 0.7, and n is from 0.6 to 1.3.

- The maximum latitudinal acceleration $mlatacc$ is less than 0.7 g and larger than 0.06 g.
- The arrival time of the maximum latitudinal position ranges from 2 s to 7 s.

Fig. 6(a) shows the available parameters under the restrictions. Fig. 6(b) shows the maximum latitudinal position and the arrival time of the available parameters. Fig. 7(a) and (b) shows the generated lane-change trajectories with two types of

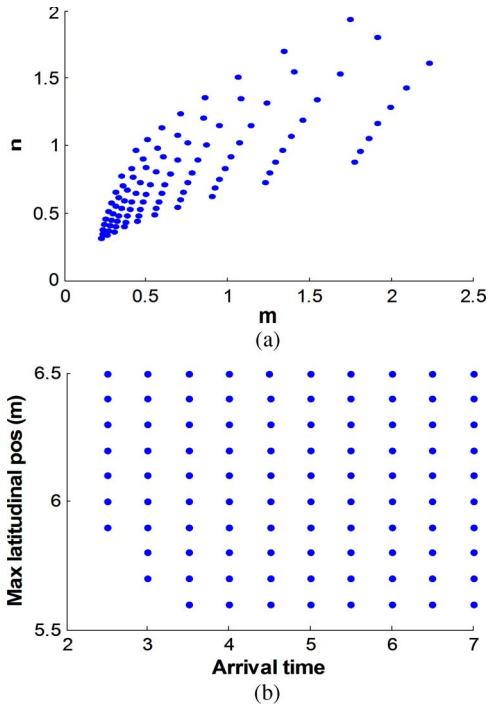

Fig. 8. Model's parameters based on different maximum latitudinal positions and the arrival time. (a) Distribution of the model's parameters. (b) Maximum latitudinal position and the arrival time.

parameters. The results show that the parameter m controls the change of lane-change trajectories at the start stage, and the parameter n adjusts the trajectories at the latter stage.

We also generate lane-change trajectories according to different maximum latitudinal positions and the arrival time. When the maximum latitudinal position and the arrival time are fixed, we can compute the model's parameters by (14) and (15). Combining with the proposed restrictions, the distribution of the model's parameters and their features is shown in Fig. 8.

D. Extended Dynamic Model

For evasive lane-change behavior, the first goal of lane change is to drive the vehicle away from dangerous areas. At the first stage of an evasive lane-change maneuver, the latitudinal acceleration rapidly increases, and the duration of this stage is long, even when the vehicle approaches the center of the destination lane. After the vehicle has left the dangerous area, the driver controls the vehicle to steadily move in the current lane.

When a vehicle or an obstacle is in front of the test vehicle in the current lane, the evasive lane-change behavior follows a lane-keeping behavior to avoid possible collisions. The destination lane of evasive lane-change behavior is a safe adjacent lane.

When a vehicle is in the destination lane behind the test vehicle and the test vehicle implements a normal lane-change behavior, the evasive lane-change behavior follows a normal lane-change behavior to avoid the collision. The destination lane of evasive lane-change behavior is the initial lane of the normal lane-change behavior.

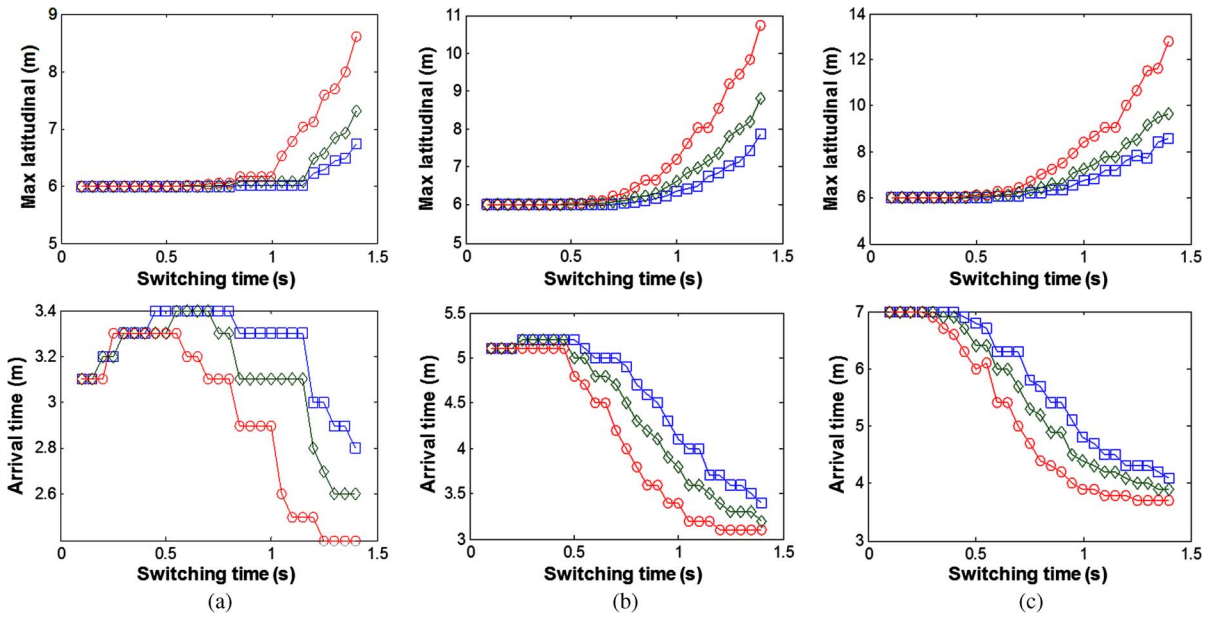

Fig. 9. Maximum latitudinal position and the arrival time of the extended dynamic model. The square line's maximum latitudinal acceleration and change rate are 0.4g and 0.4g/s, respectively. The diamond line's maximum latitudinal acceleration and change rate are 0.5g and 0.5g/s, respectively. The circle line's maximum latitudinal acceleration and change rate are 0.7g and 0.7g/s, respectively. (a) [6 m, 3 s]. (b) [6 m, 5 s]. (c) [6 m, 7 s].

In [20], the evasive lane-change model is proposed to be a combination of sinusoidal and trapezoidal models. The core idea of the method is that it divides the evasive lane-change process into two stages. Each stage is represented by different functions. Following the idea, we extend the latitudinal dynamic model to a combination of a slope model and the origin dynamic model in scenario 1 as

$$ddq(t) = \begin{cases} \min(M_{latacc}, r \cdot t), & 0 < t < t_{sw} \\ m \cdot (\beta - q(t)) - n \cdot dq(t), & t \geq t_{sw} \end{cases} \quad (19)$$

where r is the change rate of latitudinal acceleration in the first stage, and t_{sw} is the switching time between the second stage. M_{latacc} is the maximum latitudinal acceleration in the first stage. According to [20] and [36], the maximum latitudinal acceleration M is from 0.4 g to 0.7 g, and the change rate of latitudinal acceleration is from 0.4 g/s to 0.7 g/s during an evasive steering maneuver.

Fig. 9 shows the change of the maximum latitudinal position and arrival time when the switching time, the maximum latitudinal acceleration, and change rate change. The values of m and n of the dynamic model are 1.453 and 1.19, 0.523 and 0.717, 0.267 and 0.512, respectively. Therefore, the maximum latitudinal position and arrival time of the origin dynamic model are 6 m and 3 s, 6 m and 5 s, and 6 m and 7 s according to (14) and (15).

When the switching time is short, the maximum latitudinal position and the arrival time of the extended dynamic model change a little compared with the original dynamic model. However, when the change rate of latitudinal acceleration is larger or m and n are small, the change of the maximum latitudinal position and the arrival time change sharper. Therefore, although the extended dynamic model more closely matches the actual evasive lane-change behavior than the original dynamic model, it is difficult for the extended dynamic model to predict the maximum latitudinal position and the arrival time. The difficulty of satisfying different restrictions of lane-change behavior by adjusting the parameters of the extended dynamic model also increases. In addition, the switching time of the extended dynamic model is hard to be decided.

E. Vehicle in the Rear Area on the Destination Lane With High Velocity

When a vehicle in the rear area on the adjacent lane moves with a significantly higher velocity than the host vehicle, we design the following four different control strategies in this situation.

- *RCS1: The driver is unaware of the vehicle in the rear area and changes lanes with the usual operation.*
- *RCS2: The driver is aware of the vehicle in the rear area. The driver waits until the vehicle exceeds the host vehicle and then changes lanes.*
- *RCS3: The driver is aware of the vehicle in the rear area. The driver will increase the longitudinal speed to reach the acceptable relative speed and distance between the two vehicles and then change lanes. During the lane change, the driver always keeps the speed stable or increases speed to make the lane change safer.*
- *RCS4: The driver is aware of the vehicle in the rear area when the drive implements a normal lane change. The driver will stop the lane change and drive the test vehicle away from dangerous areas. Finally, the test vehicle will move into a safe adjacent lane.*

RCS1 can be modeled by the origin lane-change dynamic model. RCS2 can be modeled by the origin lane-change dynamic model with a proper response time. RCS4 can be modeled by the combination of the original and extended dynamic models for normal and evasive lane-change behaviors.

For RCS3, when the acceptable relative distance and velocity are not reached, the longitudinal dynamic model before lane change is given by

$$dds(t)=\begin{cases}\min(M_{lonacc}, aptrv/t_{dura}), & \text{if relative velocity} \\ & <aptrv \\ 0, & \text{else}\end{cases} \tag{20}$$

where M_{lonaec} is the maximum longitudinal acceleration, t_{dura} is the speedup duration reaching the acceptable relative speed, and $aptrv$ is the acceptable relative velocity between the two vehicles. In [6], the acceptance relative speed of lane-change behavior is 0–15 km/h.

The acceptable relative distance $aptrd$ is computed based on the gap acceptance model in [36]. It is given by

$$\begin{aligned} d_{crit} &= V_r^2/2M_{londec} + V_r \cdot sp \\ aptrd &= F \cdot d_{crit} \end{aligned} \tag{21}$$

where V_r is the vehicle's speed in the rear area, M_{londec} is the maximum longitudinal deceleration, sp is the car-following sensitivity parameter, d_{crit} is the distance below which the car following would be unsafe, and F is the gap adjustment factor.

Once the acceptable relative speed and acceptable relative distance are both reached, lane change occurs. In the simulation, the latitudinal speed is always zero before lane change. When lane change starts, the dynamic model switches into the origin lane-change dynamic model.

V. Trajectory Planning and Collision Prediction

The classic trajectory planning method is a close-loop optimistic process between the trajectory generator and the collision detector. The planned paths not only should be safe but is also the optimal path in the predefined conditions such as the shortest length, the minimum acceleration jerk, and the minimum energy consumption. The TTC is widely used and studied for collision prediction and risk assessment. It presents clear physical meanings and is easy to understand. Therefore, to increase real-time performance and generate collision warnings according to driver usage, we apply the multicircle contour used in [22] to compute the TTC and minimum gaps for predicting collisions.

A. Generic Dynamic Model and Collision Detector

In [27], the different traffic participants are defined by different differential equations. To take into account all the traffic participants' behavior on the road, we construct a generic dynamic model to simulate the behavior of the other traffic participants during lane change, and the differential equation of the other traffic participants is

$$\begin{bmatrix} q(n) \\ s(n) \\ dq(n) \\ ds(n) \end{bmatrix} = \begin{bmatrix} q(n-1) + dq(n-1) \cdot \Delta t \\ s(n-1) + ds(n-1) \cdot \Delta t \\ dq(n-1) + ddq(n-1) \cdot \Delta t \\ ds(n-1) + dds(n-1) \cdot \Delta t \end{bmatrix}. \tag{22}$$

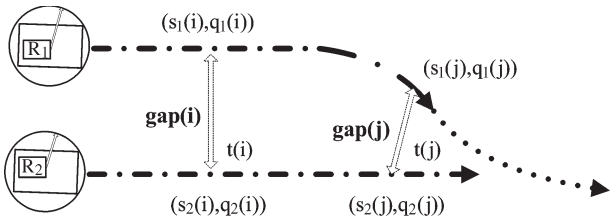

Fig. 10. Gap and TTC.

When the driver changes lane within 3–7 s, we assume that other traffic participants are in motion, with constant acceleration or deceleration. The combination of the inertial measurement unit (IMU) and RTK-DGPS can provide more accurate estimation of the longitudinal and latitudinal speed and acceleration of all the traffic participants. For example, the acceleration of static obstacles is zero, and the shape of a pedestrian is a circle with a 0.5-m radius. The path of the traffic participants is generated for 7 s.

According to (11), the discrete state equation of the test vehicle during the lane change is

$$\begin{bmatrix} q(n) \\ s(n) \\ dq(n) \\ ds(n) \end{bmatrix} = \begin{bmatrix} q(n-1) + dq(n-1) \cdot \Delta t \\ s(n-1) + ds(n-1) \cdot \Delta t \\ dq(n-1) + (m \cdot (\beta - q(n-1)) - n \cdot dq(n-1)) \cdot \Delta t \\ ds(n-1) - p \cdot dq(n-1) \cdot \Delta t \end{bmatrix}. \tag{23}$$

We describe the test vehicle or other traffic participants with one or two circles of radius R. More circles can be used to compactly enclose the vehicles, as shown in [22].

In Fig. 10, each point $(s(i), q(i))$ of the two trajectories should hold the following equations:

$$\begin{aligned} &gap(i) = \sqrt{(q_1(i) - q_2(i))^2 + (s_1(i) - s_2(i))^2}, i = 1, 2 \ldots \\ &minimum\_gap = min(gap) \\ &minimum\_gap > R_1 + R_2. \end{aligned} \tag{24}$$

When the minimum gap of two trajectories is larger than the collision gap $R_1 + R_2$, the TTC is infinite ∞, and the minimum gap of the two trajectories is computed.

When the minimum gap of two trajectories is less than the collision gap $R_1 + R_2$, the minimum gap is 0. The time of the pairwise points whose gap is less than the collision gap $R_1 + R_2$ is the TTC.

The whole step of generating safe lane-change trajectories for the lane-change module is described as follows.

1) At the beginning of the lane change, the driver attempts to plan lane-change trajectories and then activates the lane-change module. In this stage, the initial value and restrictions of the dynamic model's parameters for all the related traffic participants are provided. The driver's driving style and the layout of the road are taken into account.
2) The traffic environment surrounding the test vehicle is detected, and the module will generate driving trajectories of all the traffic participants. The generated trajectories that may cause collision with the other participants will

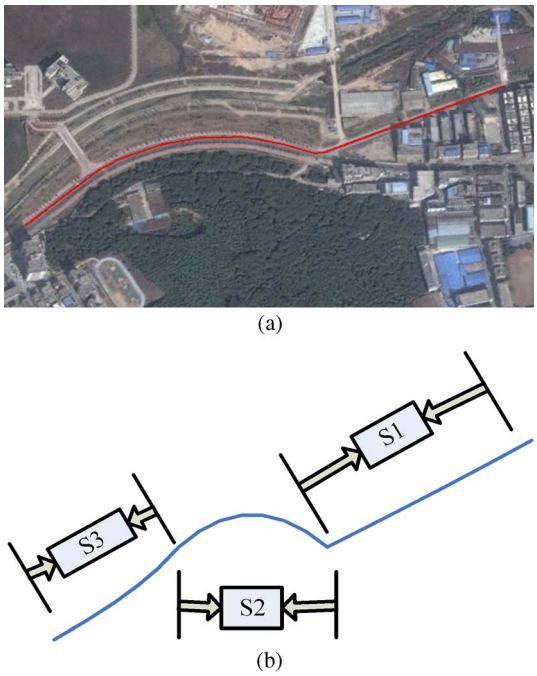

Fig. 11. Experiment track and sections. (a) Track. (b) Sections.

be removed. In this stage, the state of test vehicle and other traffic participants are updated, and the trajectories are timely regenerated.

3) Several safe trajectories with high TTC and minimum gap are shown, and the driver will change lane according to one of these trajectories. If the safe lane-change trajectories cannot be found or these trajectories do not match the driver expectation, the warning module will give the collision alarm according the TTC and minimum gap of the generated trajectories.

VI. Experiments

The goal of these experiments is to see the following two conditions:

1) how well the proposed models can fit real lane-change trajectories compared with the conventional trajectory planning method, i.e., the fifth-order polynomial model;
2) how the lane-change module plans safe and feasible lane-change trajectories for different scenes in real applications.

A. Experimental Setup

The bird's eye view of test tracks and sections are showed in Fig. 11. The track is composed of straight and curvy sections. The length of the track is 734 m, and the width of the lane is $3.75 * 2$ m. We make a road digital map ourselves and obtain the road curve and position using the RTK-DGPS receiver.

When the test vehicle moves along one lane with the speed 20–65 km/h, the driver will change lane in the section S1 and S3. In Fig. 12, we have the following two predefined lane-change scenarios for collecting the data.

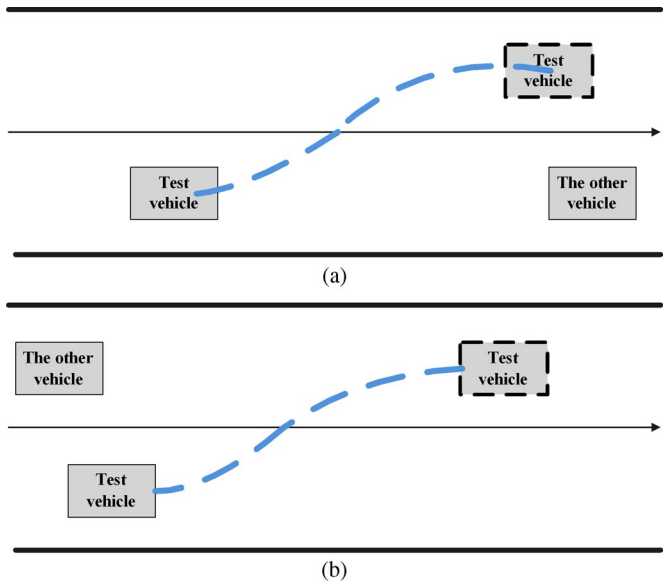

Fig. 12. Lane-change behavior scenarios. (a) Scenario 1. (b) Scenario 2.

- Scenario 1. There is a static obstacle in front of the test vehicle in the current lane. The driver will change lanes to avoid a collision with different relative speed and distance.
- Scenario 2. A vehicle moves on the destination lanes. The test vehicle speed is lower than the other vehicle. The test vehicle will change lanes into the destination lane.

After the test vehicle has moved into the destination lane, the driver is requested to keep the test vehicle moving in the middle of the current lane. It means that the target latitudinal position is about 5.5–5.65 m.

We invite six drivers to attend the experiments and collect their driving data on the scenarios. Each driver is required to drive the vehicle on the lane after the driver gets used to the test vehicle and the tracks for a period of time.

The drivers will implement lane-change behavior with the following two driving styles.

- Careful: Keep the lane change safe and comfortable.
- Aggressive: Keep the lane change safe. The initial distance between the other traffic participants and the test vehicle should be as short as possible when the lane change starts.

The drivers mark all the time slices of lane-change data according to the recorded data and video.

B. Actual Lane-Change Trajectories

Fig. 13 shows some samples of actual lane-change trajectories and the distribution of the models' parameters by fitting the actual lane-change trajectories using the original dynamic model. These samples show that lane-change behavior lasts 3–7 s. When the test vehicle arrives in the middle of the destination lane, the latitudinal speed is not zero, and the vehicle moves away from the target latitudinal position for almost all the samples.

Compared with the parameter distribution shown in Fig. 7(a) and (b), the fitted model parameters do not exceed the boundaries of the model parameters generated by the predefined restrictions in Section IV-C. Therefore, we can easily remove

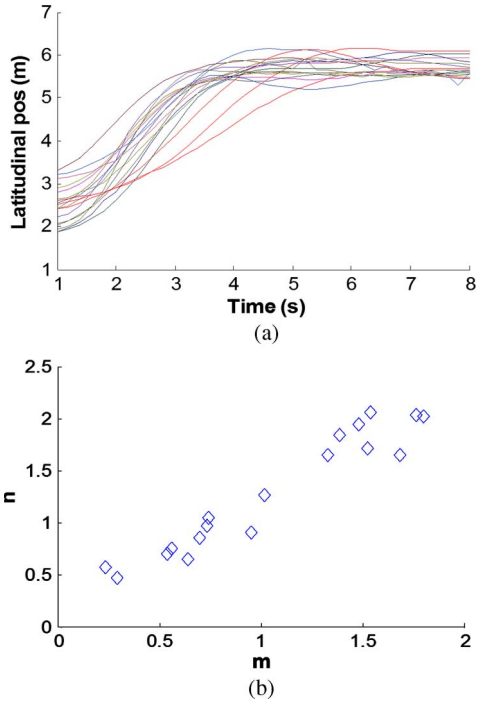

Fig. 13. Dynamic models of fitting the actual trajectories. (a) Latitudinal position of real lane-change trajectories. (b) Distribution of the fitted models' parameters.

numerous infeasible trajectories before generating the feasible trajectories by defining the range of model parameters beforehand.

C. Comparison

We compare the two dynamic models with the fifth-order polynomial model. In [22], the latitudinal position of the fifth-order polynomial model is defined as

$$q(t) = b_5 t^5 + b_4 t^4 + b_3 t^3 + b_2 t^2 + b_1 t^1 + b_0 \qquad (25)$$

where b_0–b_5 are computed according to the initial and final latitudinal states of the vehicle. In the comparison, the final latitudinal states of the test vehicle for the fifth-order polynomial model is

$$(q_{final}, dq_{final}, ddq_{final}) = (5.5, 0, 0). \qquad (26)$$

The initial latitudinal states of the vehicle are obtained based on the actual trajectories. When the vehicle arrives at the target latitudinal position, the vehicle will move with the fixed latitudinal position in the fifth-order polynomial model. We compute the arrival time of reaching the target latitudinal position of the fifth-order polynomial model by minimizing the least mean square between the actual and the generated trajectories. The switching time and the change rate of latitudinal acceleration for the extended dynamic model are also computed by minimizing the least mean square between the actual and the generated trajectories.

Fig. 14 shows the comparison of latitudinal position and acceleration among the models. Although the maximum latitudinal acceleration of the fifth-order polynomial model is smaller

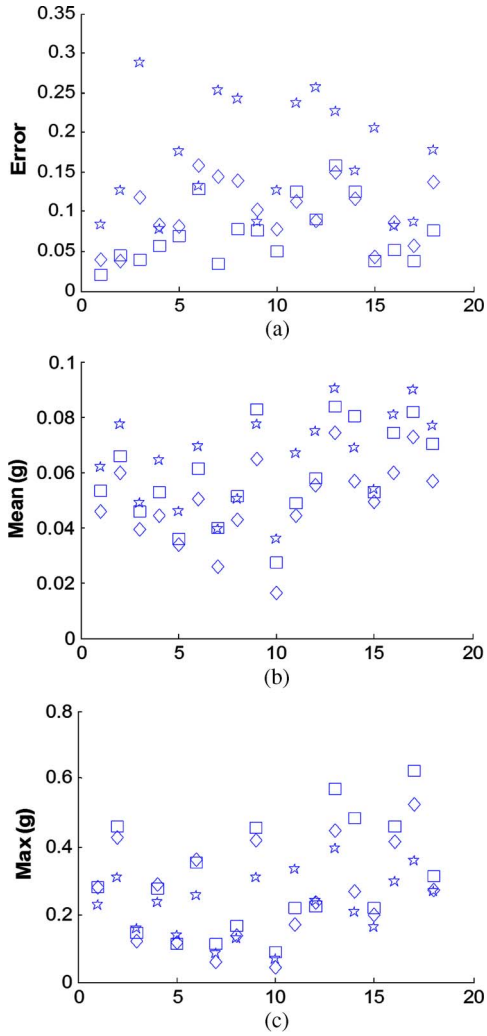

Fig. 14. Comparisons of models. The diamond represents the original dynamic model. The square represents the extended dynamic model. The pentagram represents the fifth-order polynomial model. (a) Latitudinal position error. (b) Mean of latitudinal acceleration. (c) Maximum latitudinal acceleration.

than the dynamic models for most of the generated trajectories shown in Fig. 14(c), the latitudinal position error of the fifth-order polynomial model is larger than the two dynamic models shown in Fig. 14(a).

In Fig. 14(a), the latitudinal position error of the extended dynamic model is a little better than the error of the original dynamic model. However, the difference between two dynamic models is small. The difference between the maximum and the mean latitudinal acceleration is also small. Considering that the switching time of the extended model is hard to define and that the maximum latitudinal position and the arrival time are also hard to compute, the original dynamic model is better than the extended dynamic model for lane-change trajectory planning.

D. Simulations for Lane-Change Scenarios

To analyze the parameters' boundary, which sets apart the safe, danger, and collision zones, we analyze two lane-change scenarios (defined in Section VI-A) with some pertinent predefined values of certain variables of the traffic participants and environment.

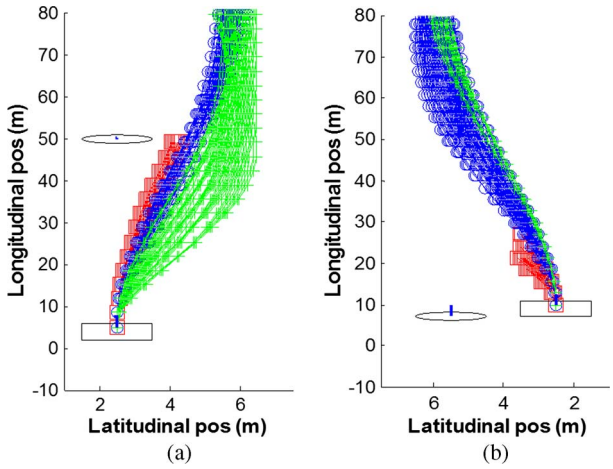

Fig. 15. Generated trajectories. The test vehicle is in a square shape, whereas the other traffic participants are in a circle shape. (a) Scenario l. (b) Scenario 2.

In scenario l, the test vehicle's speed is faster than the leading vehicle. The relative distance between the test and the leading vehicles is 50 m, and the relative speed between two vehicles is 60 m/h. The two vehicles will be in the same longitudinal position in 3 s.

In scenario 2, the test vehicle's speed is slower than the other vehicle. The relative distance between the test vehicle and the other vehicle is 3.33 m, and the relative speed between the two vehicles is l0 km/h. The two vehicles will be in the same longitudinal position in l s. The rearward vehicle on the adjacent lane is possible to be located in the blind spots of the test vehicle. The driver is unaware of the vehicle in the rear area before the lane change.

In two scenarios, we generate multiple lane-change trajectories to find the safe trajectories and compute the percentage of safe trajectories in the entire generated trajectories. We choose different parameters according to their maximum latitudinal position and the arrival time. The parameter distribution of the chosen parameters and their features are shown in Figs. 8, 16, and 17.

In the simulation, the red lane-change trajectories are the collision trajectories whose minimum gap is less than collision gap. The green lane-change trajectories are the safe trajectories whose minimum gap is large than the safe gap. The blue lane-change trajectories are the trajectories whose minimum gap is between the safe and the collision gaps. Here, the safe gap is set to larger than 2.5 m. The collision gap is set to less than 2 m.

Generated Trajectories: Fig. 15 show the generated trajectories in two scenarios.

Distribution of Model Parameters of the Trajectories: Fig. 16 shows the model parameters' distribution of the generated trajectories and refers to the percentage of safe, dangerous, and collision trajectories. In scenario l, the parameter m of safe trajectories is high. In scenario 2, the parameter n of safe trajectories is low. The percentage of safe trajectories in all trajectories can be a good indicator of estimating the severity level of the current situation for the warning module. However, the boundaries among safe, dangerous, and collision trajectories are not easily found according to the dynamic model's parameter distribution.

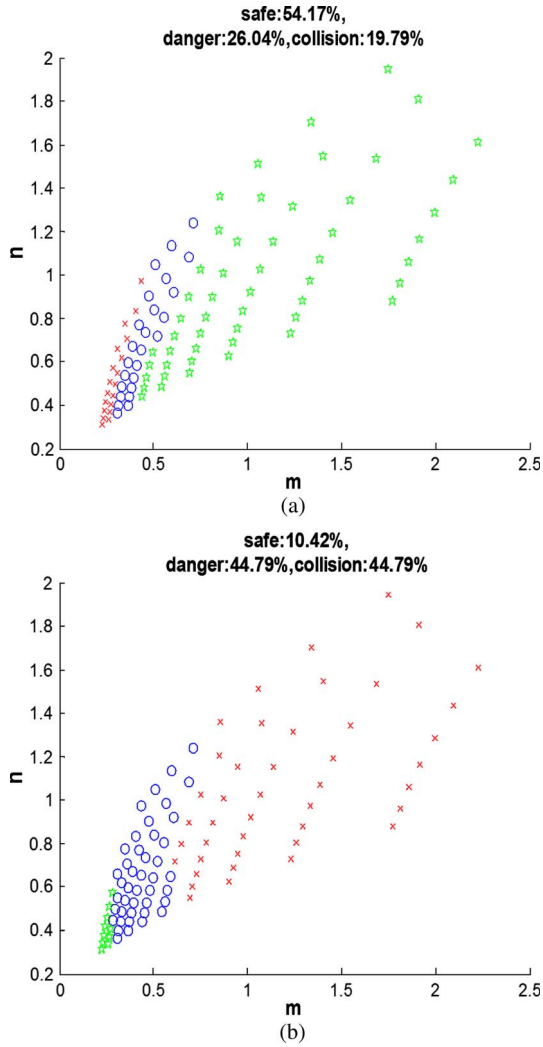

Fig. 16. Parameter distribution of two scenarios. The green-star points are safe trajectories, the blue-circle points are danger trajectories, and the red-cross points are collision trajectories. (a) Scenario l. (b) Scenario 2.

Fig. 17 shows the maximum latitudinal position and the arrival time of the generated trajectories. In scenario l, the arrival time of the maximum latitudinal position of safe trajectories is usually short. In scenario 2, the arrival time of the maximum latitudinal position of the safe trajectories is usually long.

Therefore, the maximum latitudinal position and the arrival time can be good indicators of roughly estimating the boundary of safe lane-change trajectories.

Percentage of Safe Trajectories: Fig. 18 shows the change of the percentage of safe trajectories when the relative speed and time change in the two scenarios. The relative time is computed by the relative longitudinal distance and the relative speed between the test vehicle and the other traffic participants, i.e.,

$$relative\_time = relative\_dist/relative\_speed. \quad (27)$$

Fig. 18 shows that the safe trajectories rapidly decrease when the relative time is less than 3.5 s in scenario 1. There are few safe trajectories when the relative time is less than 1.8 s. Fig. 16(b) shows that the safe trajectories rapidly decrease

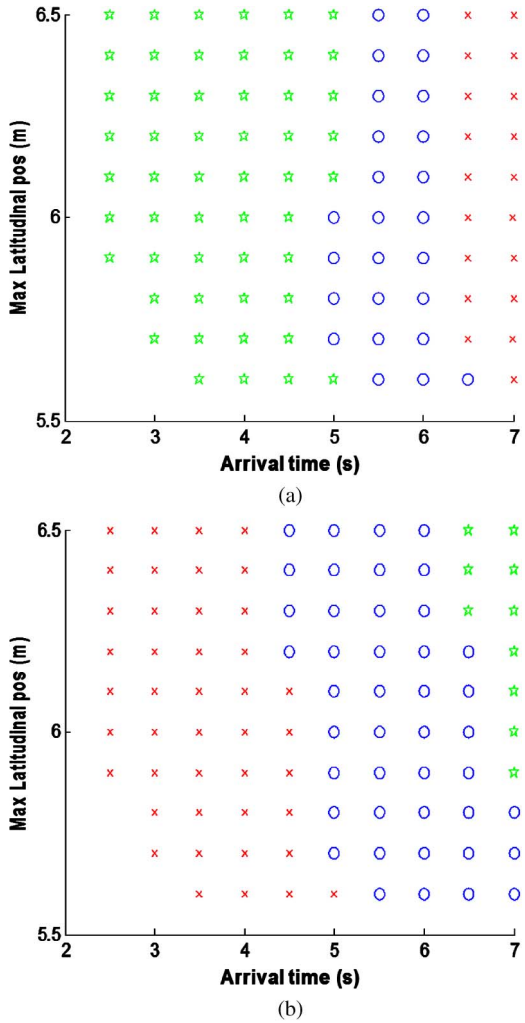

Fig. 17. Maximum latitudinal position and the arrival time. The green-star points are safe trajectories, the blue-circles points are danger trajectories, and the red-cross points are collision trajectories. (a) Scenario l. (b) Scenario 2.

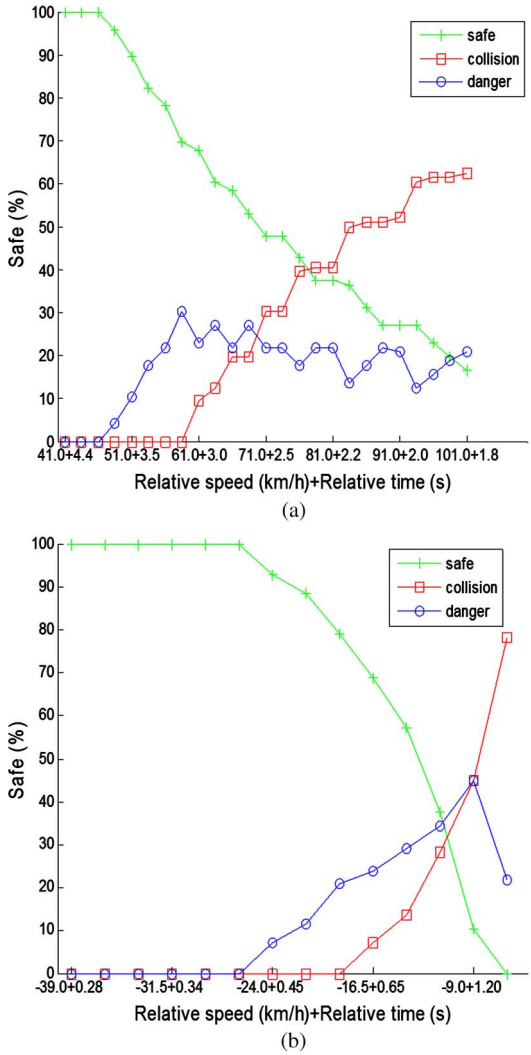

Fig. 18. Change of the percentage of safe trajectories. (a) Scenario l. (b) Scenario 2.

when the relative time is larger than about 0.4 s in scenario 2. There are few safe trajectories when the relative time is larger than 0.6 s.

We can see that the lane-change behavior may be dangerous when the other vehicle moves close to the leading vehicle. When the relative time is large than 0.6 s in scenario 2, the danger level of lane-change behavior is always extremely high.

Maximum Response Time: The response time t_m is a key variable of lane-change warning systems [20]. t_m comprises the following two indices: 1) the system delay time t_{sd} and 2) the driver reaction time t_{dr}. We have

$$t_m = t_{sd} + t_{dr}. \tag{28}$$

When the driver reaction time is about 1.38 s, 96% of the driver's steering reaction time should be faster than the time [20]. In our system, the vehicles' state updates every 0.2 s. The time of generating the trajectories and checking the collision is about 0.l–0.2 s. Therefore, the system delay time is about 0.3–0.4 s. The maximum response time is about l.7–1.8 s.

Fig. 19 shows the change of the percentage of safe trajectories with different response times.

E. Generating Safe Trajectories When the Vehicle Is in High Relative Speed

For lane-change scenarios, the highest risk comes from considerable relative velocities between the vehicles.

In Fig. 20, we apply the original and extended dynamic models to generate the safe lane-change trajectories when the vehicle should avoid the collision with the leading vehicle. In this situation, the test vehicle's speed is faster than the leading vehicle. The relative distance between the test and the leading vehicles is 33.3 m, and the relative speed between two vehicles is 60 m/h. The two vehicles will crash in about 2 s.

In Fig. 20(a), the percentage of safe, danger, and collision trajectories are 28.13%, 71.87%, and 0%, respectively, using the extended dynamic model.

In Fig. 20(b), the percentage of safe, danger, and collision trajectories are 27.08%, 18.75%, and 54.17%, respectively, using the original dynamic model.

The result shows that the extended dynamic model can decrease numerous collision trajectories in this situation.

In Fig. 21, we apply the control strategies RCS1 and RCS4 to generate the safe lane-change trajectories when the other

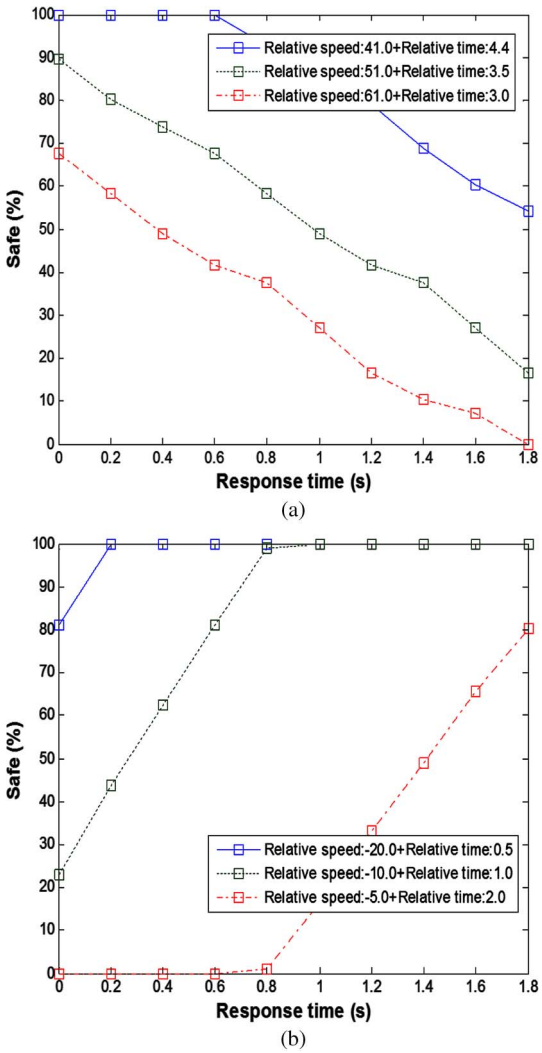

Fig. 19. Percentage of safe trajectories with different response times. (a) Scenario 1. (b) Scenario 2.

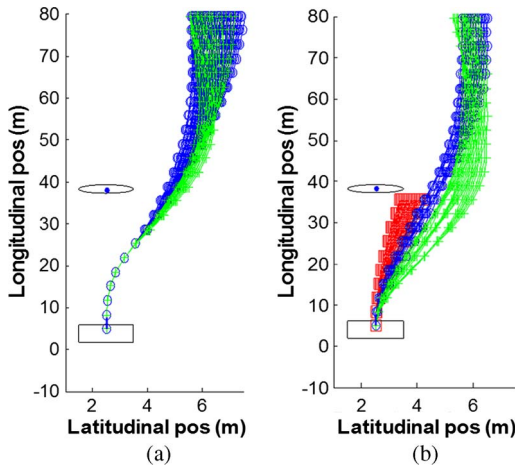

Fig. 20. Generated safe trajectories when the vehicle is in the front area. The maximum latitudinal acceleration and change rate are 0.4 g and 0.4 g/s, respectively. (a) Extend dynamic model. (b) Original dynamic model.

vehicle is in the rear area. In this situation, the test vehicle's speed is slower than the other vehicle. The relative distance between the test vehicle and the other vehicle is 55.5 m, and

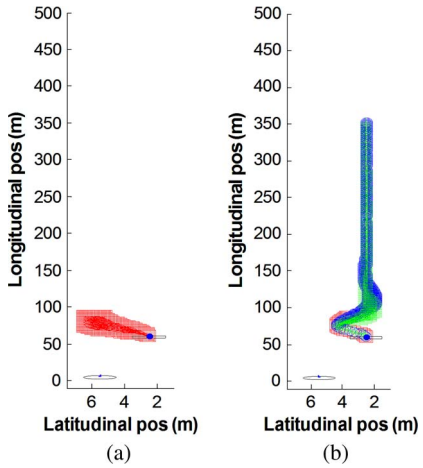

Fig. 21. Generated safe trajectories using RCS1 and RCS4. (a) RCS 1. (b) RCS4.

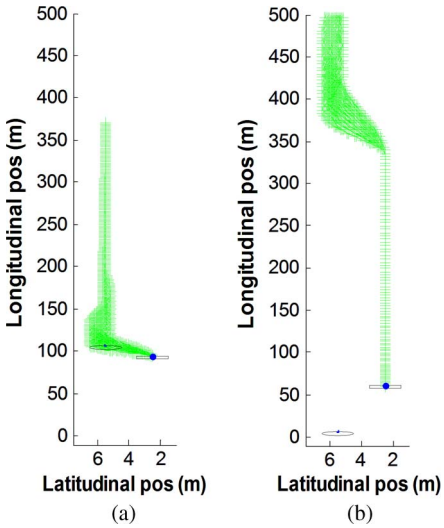

Fig. 22. Generated safe trajectories using RC2 and RC3. The waiting time of RCS2 is 6 s. $aptrd$ is 25.7 m, and $aptrv$ is 10 km/h. t_{dura} is 5 s. (a) RCS2. (b) RCS3.

the relative speed between two vehicles is 40 km/h. The two vehicles will be in the same longitudinal position in 5 s.

In Fig. 21(a), the generated trajectories are all collision trajectories. In Fig. 21(b), the percentage of safe, danger, and collision trajectories are 59.38%, 33.33%, and 7.29%, respectively. The switching time from the original dynamic model to the extended dynamic model is 1.38 s. tsw, M_{latacc}, r, m, and n of the extended dynamic model are 1, 0.2 g, 0.2 g/s, 0.523, and 0.717, respectively.

In Fig. 22, we apply the control strategies RCS2 and RCS3 in the same scenario with Fig. 22. In Fig. 22, the results show that the generated trajectories are all safe trajectories. The simulation results shows that the proposed dynamic model can effectively emulate different lane-change strategies and plan the safe trajectories.

F. Field Test

To increase the real-time performance of the lane-change module in the field test, the lane-change module is running on an Intel 2.4-GHz Core i3 laptop computer. The lane-change

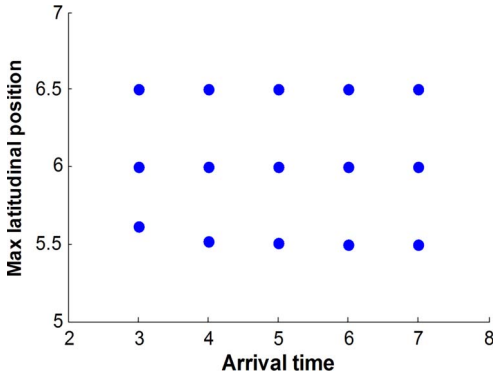

Fig. 23. Maximum latitudinal position and the arrival time of the maximum latitudinal position.

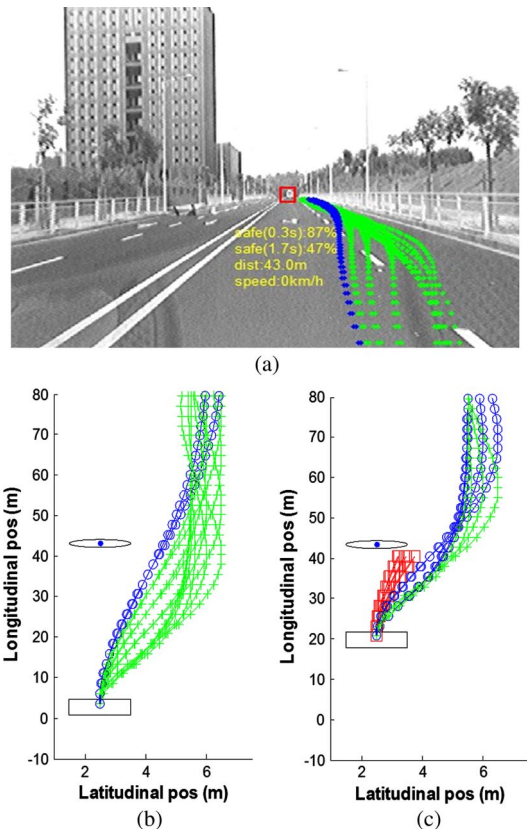

Fig. 24. Field test 1. (a) Vehicle is in front of the test vehicle in the same lane. (b) Response time is 0.3 s. (c) Response time is 1.7 s.

module will timely generate only 15 lane-change trajectories when the turn signal is activated. The maximum latitudinal position and arrival time of generated trajectories are shown in Fig. 23. The time of generating the trajectories is 0.1 s using the second- and third-order Runga–Kutta–Fehlberg. Figs. 22 and 23 show the field tests in the experiments. The test vehicle's speed is 20–60 km/h. All the experiments happened in S1 of the track, and the vision is clear. The percentage of safe trajectories is computed with different response times (0.3 and 1.7 s).

In field test 1 (see Fig. 24), the test vehicle's speed is 44 km/h, and the leading vehicle's speed is 0 km/h. The distance is 43 m between the two vehicles.

In field test 2 (shown in Fig. 25), the test vehicle's speed is 41 km/h, and the speed of the other vehicle in the rear area

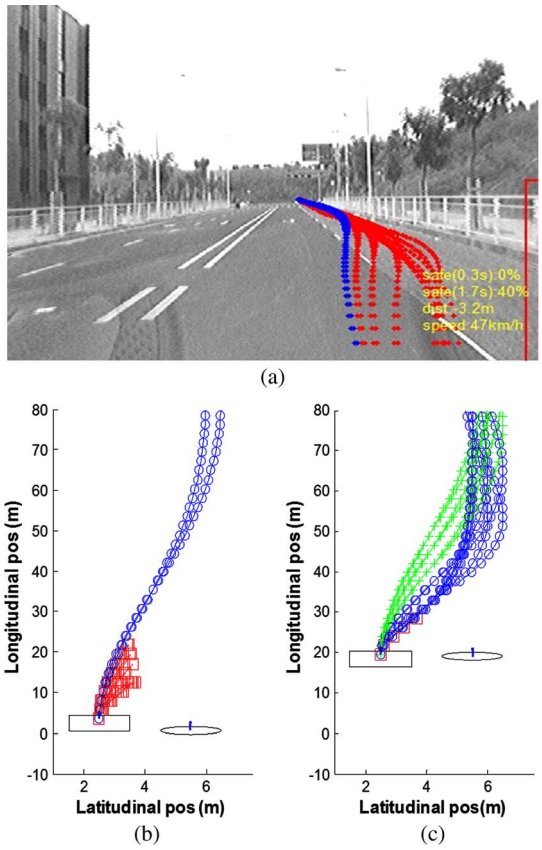

Fig. 25. Field test 2. (a) Vehicle is behind the test vehicle in the other lane. (b) Response time is 0.3 s. (c) Response time is 1.7 s.

on the adjacent lane is 47 km/h. The relative distance is 3.2 m between the two vehicles.

VII. Conclusion

The core result of this paper has been the modeling of the driver control strategy of lane-change behavior and planning the trajectories using the dynamic models in the driver-assistance system. We describe the function of the lane-change module in the driver-assistance system and the principle that governs the lane-change dynamic model. Based on the control strategies of lane-change behavior, we have proposed the lane-change dynamic models and provided appropriate lane-change trajectories. We also analyzed the features of the latitudinal dynamic model and presented the methods for computing the maximum latitudinal position and arrival time. Furthermore, we put forward an extended dynamic model to represent the control strategy of evasive lane-change behavior.

Compared with the fifth-order polynomial lane-change method, the dynamic models fit actual lane-change trajectories better and can generate more accurate lane-change trajectories. Furthermore, the dynamic model can represent different driving styles (such as slow and careful, as well as sudden and aggressive) by using different model parameters.

We apply the dynamic models in emulating different lane-change strategies and predicting lane-change trajectories for collision prediction. We use the models to compute the percentage of safe trajectories in different lane-change scenarios and assess the effect of the response time on the percentage

of safe trajectories. The simulation shows that the maximum latitudinal position and arrival time of the generated lane-change trajectories can be good indicators of safe lane-change trajectories when the other relative variables of the traffic participants are fixed or estimated. In the field test, the dynamic models can generate the feasible lane-change trajectories and efficiently compute the percentage of safe trajectories. The proposed methods and module can be combined with the human–machine interface to help the driver easily identify safe lane-change trajectories and areas.

The experiments also show several limitations of the proposed method. First, the lane-change trajectory planning heavily depends on high-accuracy GPSs, and the latitudinal positions of the vehicles entirely depend on the local digital map and the RTK-DGPS receiver. If there are high buildings or trees along the test road, the measurement error of the vehicle state is sometimes large, and the generated lane-change trajectories are incorrect. Second, the appropriate traffic participants' behavior model determines the collision prediction, particularly in a crowded traffic environment. Third, although the dynamic model can describe the different driving styles through the selection of different parameters, these parameters still cannot be applied when modeling the driving profile for driver identification. Finally, the dynamic model is unsuitable for tracks with high curvatures because of the random bias for latitudinal acceleration, which the driver adjusts for lane-keeping behavior.

In the future, we will incorporate various driving behaviors such as lane keeping, turning around a corner, and overtaking into a switch model. We also intend to develop and validate these models and methods in an actual urban environment with multiple vehicles and different road curves. Furthermore, we will integrate facial expression recognitions into the lane-change module to enhance the performance of collision prediction when the driver is affected by strong emotion.

REFERENCES

[1] R. Bishop, *Intelligent Vehicle Technology and Trends*. London, U.K.: Artech House, 2006, pp. 50–80.

[2] A. Lindgren, F. Chen, P. W. Jordan, and H. X. Zhang, "Requirements for the design of advanced driver assistance systems—The differences between Swedish and Chinese drivers," *Int. J. Des.*, vol. 2, no. 2, pp. 41–54, Aug. 2008.

[3] M. C. Nechyba and Y. S Xu, "Stochastic similarity for validating human control strategy models," *IEEE Trans. Robot. Autom.*, vol. 14, no. 3, pp. 437–451, Jun. 1998.

[4] M. C. Nechyba and Y. S. Xu, "On learning discontinuous human control strategies," *Int. J. Intell. Syst.*, vol. 16, no. 4, pp. 547–570, Apr. 2001.

[5] Y. S. Ou, H. H. Qian, and Y. S. Xu, "Support-vector-machine-based approach for abstracting human control strategy in controlling dynamically stable robots," *J. Intell. Robot. Syst.*, vol. 55, no. 1, pp. 39–54, Jun. 2009.

[6] E. C. B. Olson, "Modeling slow lead vehicle lane changing," Ph.D. dissertation, Ind. Syst. Eng., Virginia Polytechnic Inst., Blacksburg, VA, 2003.

[7] P. G. Gipps, "A model for the structure of lane-changing decisions," *Transp. Res. B: Methodol.*, vol. 20, no. 5, pp. 403–414, Oct. 1986.

[8] K. I. Ahmed, "Modeling drivers' acceleration and lane changing behavior," Ph.D. dissertation, Mass. Inst. Technol., Cambridge, MA, 1999.

[9] A. Kesting, M. Treiber, and D. Helbing, "General lane-changing model MOBIL for car-following models," *Transp. Res. Rec.*, vol. 1999, no. 1, pp. 86–94, 2007.

[10] N. Oliver and A. P. Pentland, "Graphical models for driver behavior recognition in a SmartCar," in *Proc. IEEE Intell. Veh. Symp.*, 2000, pp. 7–12.

[11] M. H. Mandalia and D. D. Salvucci, "Using support vector machines for lane-change detection," in *Proc. 49th Annu. Meet. Hum. Factor Ergonom. Soc.*, 2005, pp. 1965–1969.

[12] D. D. Salvucci, H. M. Mandalia, N. Kuge, and T. Yamamura, "Lane-change detection using a computational driver model," *Hum. Factors*, vol. 49, no. 3, pp. 532–542, Jun. 2007.

[13] J. C. McCall, D. P. Wipf, M. M. Trivedi, and B. D. Rao, "Lane change intent analysis using robust operators and sparse Bayesian learning," *IEEE Trans. Intell. Transp. Syst.*, vol. 8, no. 3, pp. 431–440, Sep. 2007.

[14] A. Pentland and A. Liu, "Modeling and prediction of human behavior," *Neural Comput.*, vol. 11, no. 1, pp. 229–242, Jan. 1999.

[15] D. D. Salvucci, "Modeling driver behavior in a cognitive architecture," *Hum. Factors*, vol. 48, no. 2, pp. 362–380, Summer 2006.

[16] J. H. Kim, S. Hayakawa, T. Suzuki, K. Hayashi, S. Okuma, N. Tsuchida, M. Shimizu, and S. Kido, "Modeling of driver's collision avoidance maneuver based on controller switching model," *IEEE Trans. Syst., Man, Cybern. A: Syst., Humans*, vol. 35, no. 6, pp. 1131–1143, Dec. 2005.

[17] S. Sekizawa, S. Inagaki, T. Suzuki, S. Hayakawa, N. Tsuchida, T. Tsuda, and H. Fujinami, "Modeling and recognition of driving behavior based on stochastic switched ARX model," *IEEE Trans. Intell. Transp. Syst.*, vol. 8, no. 4, pp. 593–606, Dec. 2007.

[18] N. Sledge and K. Marshek, "Comparison of ideal vehicle lane-change trajectories," *Res. Veh. Dynam. Simul.*, vol. 971062, pp. 233–256, 1997.

[19] K. Enke, "Possibilities for improving safety within the driver vehicle environment control loop," in *Proc. 7th Int. Tech. Conf. Exp. Safety Veh.*, 1979, pp. 789–802.

[20] J. D. Chovan, "Examination of lane change crashes and potential IVHS countermeasures," Nat. Hwy. Traffic Safety Admin., Dept. Transp., Washington, DC, Tech. Rep. DOT HS 808 071, 1994.

[21] W. Nelson, "Continuous-curvature paths for autonomous vehicles," in *Proc. IEEE Int. Conf. Robot. Autom.*, 1989, pp. 1260–1264.

[22] I. Papadimitriou and M. Tomizuka, "Fast lane changing computations using polynomials," in *Proc. Amer. Control Conf.*, 2003, pp. 48–53.

[23] J. L. Bascunana, "Analysis of lane-change crash avoidance," *SAE Tech. Paper Ser.*, vol. 951895, pp. 33–41, Aug. 1995.

[24] H. Jula, E. B. Kosmatopoulos, and P. A. Ioannou, "Collision avoidance analysis for lane changing and merging," *IEEE Trans. Intell. Transp. Syst.*, vol. 49, no. 6, pp. 2295–2308, Nov. 2000.

[25] D. L. Smith, R. Glassco, J. Chang, and D. Cohen, "Feasibility of modeling lane-change performance," Nat. Hwy. Traffic Safety Admin., Washington, DC, Tech. Rep. 2003-01-0280, 2003.

[26] R. Schubert, K. Schulze, and G. Wanielik, "Situation assessment for automatic lane-change maneuvers," *IEEE Trans. Intell. Transp. Syst.*, vol. 11, no. 3, pp. 607–616, Sep. 2010.

[27] A. E. Broadhurst, S. Baker, and T. Kanade, "Monte Carlo road safety reasoning," in *Proc. IEEE Intell. Veh. Symp.*, 2005, pp. 319–324.

[28] S. Rezaei and S. Raja, "Kalman-filter-based integration of DGPS and vehicle sensors for localization," *IEEE Trans. Control Syst. Technol.*, vol. 15, no. 6, pp. 1080–1088, Nov. 2007.

[29] J. Guivant, E. Nebot, and S. Baiker, "Autonomous navigation and map building using laser range sensors in outdoor applications," *J. Robot. Syst.*, vol. 17, no. 10, pp. 565–583, Oct. 2006.

[30] M. Peräaho, E. Keskinen, and M. Hatakka, "Driver competence in a hierarchical perspective—Implications for driver education," Traffic Research, Univ. Turku, Turku, Finland, Jun. 2003.

[31] S. Hetrick, "Examination of driver lane-change behavior and the potential effectiveness of warning onset rules for lane-change or 'side' crash avoidance systems," M.S. thesis, Ind. Syst. Eng., Virginia Polytechnic Inst., Blacksburg, VA, 1997.

[32] W. W. Wierwille, *Driver Steering Performance. Automotive Engineering and Litigation*. New York: Garland, 1984, ch. 16, pp. 407–434.

[33] R. E. Chandler and R. Herman, "Traffic dynamics: Studies in car following," *Oper. Res.*, vol. 6, no. 2, pp. 165–184, Mar. 1958.

[34] D. C. Gazis and R. Herman, "Nonlinear follow-the-leader models of traffic flow," *Oper. Res.*, vol. 9, no. 4, pp. 545–567, Jun. 1961.

[35] G. F. Newell, "Nonlinear effects in the dynamics of car following," *Oper. Res.*, vol. 9, no. 2, pp. 209–229, Mar. 1961.

[36] R. D. Worall and A. G. R. Bullen, "An empirical analysis of lane changing on multilane highways," *Hwy. Res. Board*, vol. 303, pp. 30–43, 1970.

[37] N. A. Webster, T. Suzuki, and M. Kuwahara, "Tactical lane change model with sequential maneuver planning," *Transportmetrica*, vol. 4, no. 1, pp. 63–78, Jan. 2008.

[38] H. S Tan and J. H. Huang, "Experimental development of a new target and control driver steering model based on DLC test data," *IEEE Trans. Intell. Transp. Syst.*, vol. 13, no. 1, pp. 375–384, Mar. 2012.

Guoqing Xu received the B.Sc., M.Sc., and Ph.D. degrees in electrical engineering from Zhejiang University, Hangzhou, China, in 1988, 1991, and 1994, respectively.

He was a Postdoctoral Researcher with the Northern Jiaotong University, Beijing, China. In 1997, he joined Tongji University, Shanghai, China, where he was an Associate Professor, later became a Professor with the Department of Electrical Engineering, and has been the Chair of the Department of Electrical Engineering since 2003. From 2006 to 2007, he was with the Department of Automation and Computer-Aided Engineering, Chinese University of Hong Kong (CUHK), Hong Kong, SAR, as a Visiting Professor. In 2007, he was an Associate Director with Shenzhen Institute of Advanced Integration Technology, Chinese Academy of Sciences (CAS)/CUHK, Shenzhen, as a Professor of mechanical and automation engineering. In 2009, he was the Chief Scientist with the R&D Centre for Electric Vehicle, CAS. Since 2010, he has been the Director of Shenzhen Institute of Advanced Integration Technology, CUHK/CAS. He has published more than 100 refereed papers in international journals and conference proceedings. His research interests include power electronics, motion control, and electric vehicle.

Li Liu received the B.S degree from the University of Xiangtan, Hunan, China, in 2004 and the M.Sc. degree from the University of Hunan, in 2007. He is currently pursuing the Ph.D. degree with the Shenzhen Institute of Advanced Integration Technology, Chinese Academy of Sciences/The Chinese University of Hong Kong, Shenzhen, China

His research interests include wheeled mobile robots, driver behavior, trajectory planning, Bayesian networks, and driver-assistance systems.

Yongsheng Ou received the B.Sc. degree in mechanical and electrical engineering from Beijing University of Aeronautics and Astronautics, Beijing, China, in 1995, the M.Sc. degree in electrical engineering from the Chinese Academy of Sciences, Shenzhen, China, in 1998, and the Ph.D. degree in automation and computer-aided engineering from the Chinese University of Hong Kong, Shatin, Hong Kong, in 2004.

He is currently a Professor with the Shenzhen Institute of Advanced Integration Technology, Chinese Academy of Sciences/The Chinese University of Hong Kong, Shenzhen. He is a coauthor of the monograph *Control of Single Wheel Robots* (Springer, 2005). His research interests include the control of complex systems, learning control by demonstration, and computer vision.

Zhangjun Song received the B.E. and M.S.E. degrees from the Northeastern University, Shenyang, China, in 1999 and 2002, respectively, and the Ph.D. degree from Tsinghua University, Beijing, China, in 2007.

Since 2007, he has been an Assistant Research Fellow with Shenzhen Institute of Advanced Integration Technology, Chinese Academy of Sciences/The Chinese University of Hong Kong, Shenzhen. His research interests include intelligent service robots and the modeling, motion planning, and control of wheeled mobile robots.